Interplay between point symmetry, oxidation state, and the Kondo effect in 3*d* transition metal acetylacetonate molecules on Cu(111)

Hongyan Chen [1,*,†] Timo Frauhammer,[1,†] Satoru Sasaki,[2] Toyo Kazu Yamada [2,3] and Wulf Wulfhekel[1]
[1]*Physikalisches Institut, Karlsruhe Institute of Technology, Wolfgang Gaede Strasse 1, 76131 Karlsruhe, Germany*
[2]*Department of Materials Science, Chiba University, 1-33 Yayoi-cho, Inage-ku, Chiba 263-8522, Japan*
[3]*Molecular Chirality Research Centre, Chiba University, 1-33 Yayoi-cho, Inage-ku, Chiba 263-8522, Japan*

(Received 18 November 2020; revised 26 January 2021; accepted 27 January 2021; published 15 February 2021)

We report that the occurrence of a Kondo effect in magnetic molecules crucially depends on the point symmetry and oxidation state of the adsorbed species. Two different transition metal acetylacetonate (acac) compounds [M(acac)$_3$, with M = Cr(III) or Co(III)] adsorbed on a Cu(111) single crystal were investigated to demonstrate the interplay. After deposition, Cr(acac)$_3$ molecules formed threefold symmetric Cr(acac)$_3$ and twofold symmetric Cr(acac)$_2$ by releasing a ligand, while Co(acac)$_3$ molecules only formed twofold symmetric Co(acac)$_2$. Threefold symmetric Cr(acac)$_3$ molecules with a total electron spin $S = \frac{3}{2}$ exhibited no Kondo effect, while a clear Kondo resonance was observed in twofold Cr(acac)$_2$ molecules. Co(acac)$_2$ molecules surprisingly showed no Kondo resonance, even in the case of twofold symmetry, which is explained by a low-spin state of $S = 0$. To analyze the results, a simple model is proposed based on the total electron spin and the symmetry of magnetic molecule. The present approach provides a feasible design strategy for single molecule magnets on metallic surfaces.

DOI: 10.1103/PhysRevB.103.085423

I. INTRODUCTION

Single molecule magnets (SMMs) have attracted much attention due to their potential application as building blocks for bits in quantum computers [1–7]. Among the different approaches toward SMMs, 3*d* transition metal-based systems have the advantage that the 3*d* orbitals are not strongly localized and even contribute to the coordinative bonds between the ligands and the central metal ion, making them readily accessible to scanning tunneling microscopy (STM) [8–11]. Further, due to the relatively strong coupling of the spins to the environment, the magnetic properties of 3*d* magnetic ions can be tuned with the help of external environment [10,12–15]. That is, both detection and manipulation of 3*d* transition metal SMMs are easily possible. For example, by modifying the point symmetry of the attached ligands, the ligand field can be varied, including the magnetic anisotropy or the zero-field splitting (ZFS) of the SMMs [16–18]. In general, the ZFS of the magnetic states can be expressed by the ligand field Hamiltonian, which consists of the sum of Stevens operators [19]. Depending on the symmetry, some terms are allowed, and others are forbidden, which gives an excellent opportunity to modify the magnetic behavior of SMMs adsorbed on conductive surface or even to develop design rules for systems [3,18,20].

In this paper, we present an experimental STM study of two different transition metal acetylacetonate compounds M(acac)$_3$ (with M = Cr or Co) on Cu(111) at low temperature. We find that Cr(acac)$_3$ molecules form two different species with twofold symmetry [Cr(acac)$_2$] or threefold symmetry [Cr(acac)$_3$] when deposited on Cu(111). Especially, the twofold symmetric Cr(acac)$_2$ molecule with a total electron spin $S = \frac{3}{2}$ of the Cr^{3+} exhibits a pronounced Kondo resonance at the Fermi level and one inelastic excitation, while for the threefold symmetric Cr(acac)$_3$, no spectral features were observed. For Co-acetylacetonate compounds, only twofold symmetric molecules [Co(acac)$_2$] were observed, showing featureless scanning tunneling spectroscopy (STS) as well. We demonstrate that, by combining the consideration of the total electron spin of magnetic ions and the point symmetry of local environment of the magnetic molecules, the observed results can be well understood by a model based on ZFS, which will be discussed later. This is essential for starting to design a SMM system.

II. EXPERIMENTAL DETAILS

The trivalent Cr and Co acetylacetonates are chelate complexes composed of three organic acac ligands such that the central metal ion is surrounded by six oxygen atoms in octahedral symmetry [21]. Figures 1(a) and 1(b) show the molecule structure and the spin configurations of the two compounds. The 3*d* orbitals split into e_g and t_{2g} orbitals in octahedral symmetry. In Cr(III)(acac)$_3$, the three remaining 3*d* electrons each occupy one of the t_{2g} orbitals and form a total spin $S = \frac{3}{2}$ [22]. In contrast, Co(III)(acac)$_3$ was reported to be diamagnetic with $S = 0$ [22], i.e., the six remaining electrons doubly occupy the t_{2g} orbitals, and the Co ion is in a low spin state. The molecules were deposited on a clean Cu(111) single crystal substrate in ultrahigh vacuum (UHV) at

*hongyan.chen@kit.edu
†These authors contributed equally to this work.

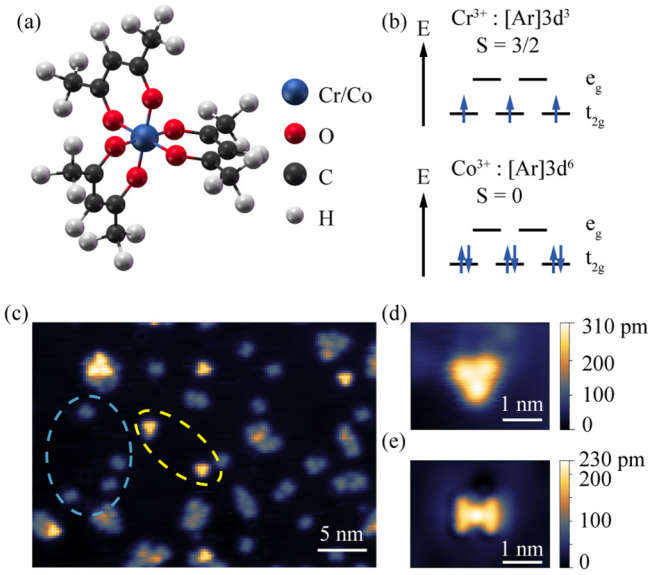

FIG. 1. (a) Molecule structure of the trivalent acetylacetonates: the molecule is a chelate complex, where the central transition metal ion (Cr or Co) is surrounded by six oxygen atoms in octahedral symmetry. (b) Simplified electronic configurations of the molecules. In the gas phase, $Cr(acac)_3$ is paramagnetic with a spin $S = \frac{3}{2}$, while the $Co(acac)_3$ is diamagnetic with $S = 0$. (c) Large-scale scanning tunneling microscopy (STM) image of Cr-acetylacetonates adsorbed on Cu(111) surface ($V = 1.0$ V, $I = 100$ pA, $T = 800$ mK). Both triangular-shaped $Cr(acac)_3$ and dumbbell-shaped $Cr(acac)_2$ molecules can be observed, which were marked by yellow and blue dashed lines, respectively. (d) and (e) are zoom-in images of $Cr(acac)_3$ and $Cr(acac)_2$ molecules, respectively. The height scales show clear height difference (about 80 pm) between the two different species.

room temperature using a homemade Knudsen cell. The UHV system is further equipped with a low temperature STM using a Joule-Thomson cooling stage with ^{3}He and an operation temperature of about 700 mK [23]. The samples were transferred to STM immediately after growth.

It has been reported that $Cr(acac)_3$ can be sublimed without molecule decomposition [24]. In this paper, however, we observed two different species of Cr-acetylacetonate molecules. More precisely, we obtained threefold symmetric molecules consisting of three lobes in triangular shape [see Fig. 1(d) and Fig. 2(b)] and twofold symmetric dumbbell-shaped molecules [see Fig. 1(e) and Fig. 2(a)] at the same time [see Fig. 1(c)] after deposition of $Cr(acac)_3$ at 62 °C and an evaporating pressure around 10^{-8} mbar. If every lobe corresponds to one individual acac ligand, then the triangles and dumbbells represent $Cr(acac)_3$ and $Cr(acac)_2$, respectively. We always observed a fraction of partially decomposed molecules.

For Co-acetylacetonate molecules, we only observed twofold symmetric molecules [$Co(acac)_2$] after deposition, even at a lower deposition temperature of only 44 °C [see Fig. 3(a)]. Indeed, we can confirm a strong tendency for partial disintegration of $Co(acac)_3$ in agreement with the literature which shows that $Co(acac)_3$ may decompose at temperatures around 220 °C, leading to the generation of divalent $Co(acac)_2$ [25,26]. Note that the dumbbell-shaped $M(acac)_2$ (M = Cr or Co) molecules could not be attributed to the different adsorption site of $M(acac)_3$ on the Cu(111) surface. A clear height difference between the triangular-shaped and the dumbbell-shaped molecules is estimated to be about 80 pm and can be extracted from Figs. 1(d) and 1(e).

III. RESULTS

To study the magnetic behavior of the 3d magnetic ions, we measured dI/dV spectra on different species of Cr-acetylacetonates at the center of the molecules. Interestingly, the two different objects show very different behavior. As shown in Fig. 2(a), the dumbbell-shaped $Cr(acac)_2$ molecules show a clear peak at the Fermi level in combination with two faint shoulders marked in blue arrows. Such sharp features on a scale of a few millielectronvolts cannot be caused by molecular orbitals but indicates a Kondo resonance. The faint shoulders can be interpreted as inelastic excitations, as will be discussed in more detail below. The triangular-shaped $Cr(acac)_3$ molecules, however, show an almost featureless spectrum, as displayed in Fig. 2(b). Note that, due to the surface state of Cu(111) and scattering of the two-dimensional electron gas by the adsorbed molecules [27], the density of states is not entirely flat, as evidenced by the spectrum recorded directly on Cu(111) [dI/dV spectra in red in Fig. 2(a) and 2(b)].

To investigate the nature of the sharp peak in the $Cr(acac)_2$ molecules, we recorded position-dependent spectra. Figure 2(c) shows the topography of the molecule with higher lateral resolution. For every pixel, the feedback loop was opened, and dI/dV spectra were recorded. Figure 2(d) displays the corresponding laterally resolved dI/dV signal at zero bias. Clearly, the resonance is in the molecule center, where the Cr ion is expected. This indicates that the resonance results from the unpaired spins of the magnetic ion rather than the ligands [9]. To better understand the resonance feature and the symmetric shoulders, we fitted the experimental spectrum with the following model function like that proposed in Ref. [28]:

$$\frac{dI}{dV}(\epsilon) = c + m\epsilon + A_K f(\epsilon, q, \Gamma_F) + A_S[\Theta(\epsilon_{ex} + \epsilon, T) + \Theta(\epsilon_{ex} - \epsilon, T)]. \quad (1)$$

The model contains a constant c, a linear background $m\epsilon$, a Fano-Frota function $f(\epsilon, q, \Gamma_F)$ [29,30], and two thermally broadened step functions $\Theta(\epsilon_{ex} \pm \epsilon, T)$ with

$$\Theta(x) = \frac{1 + (x-1)\exp(x)}{[\exp(x) - 1]^2} \quad \text{and} \quad x = \frac{\epsilon}{k_B T}, \quad (2)$$

describing indirect tunneling through the Kondo cloud and interference with direct tunneling to the substrate, as well as inelastic excitations. Figure 2(e) shows the fitting results; the experimental data were plotted in black and the result of the fit in red. The fitting function reproduces very well all details of the experimental spectrum. The fit gives an estimated half-width at half-maximum (HWHM) of the Kondo peak of $\Gamma_F = (1.69 \pm 0.02)$ meV and an excitation energy of $\epsilon_{ex} = (0.76 \pm 0.03)$ meV. This can be more easily recognized from the inset of Fig. 2(e), which shows the fitting resonance in blue and the inelastic steps in orange, sepa-

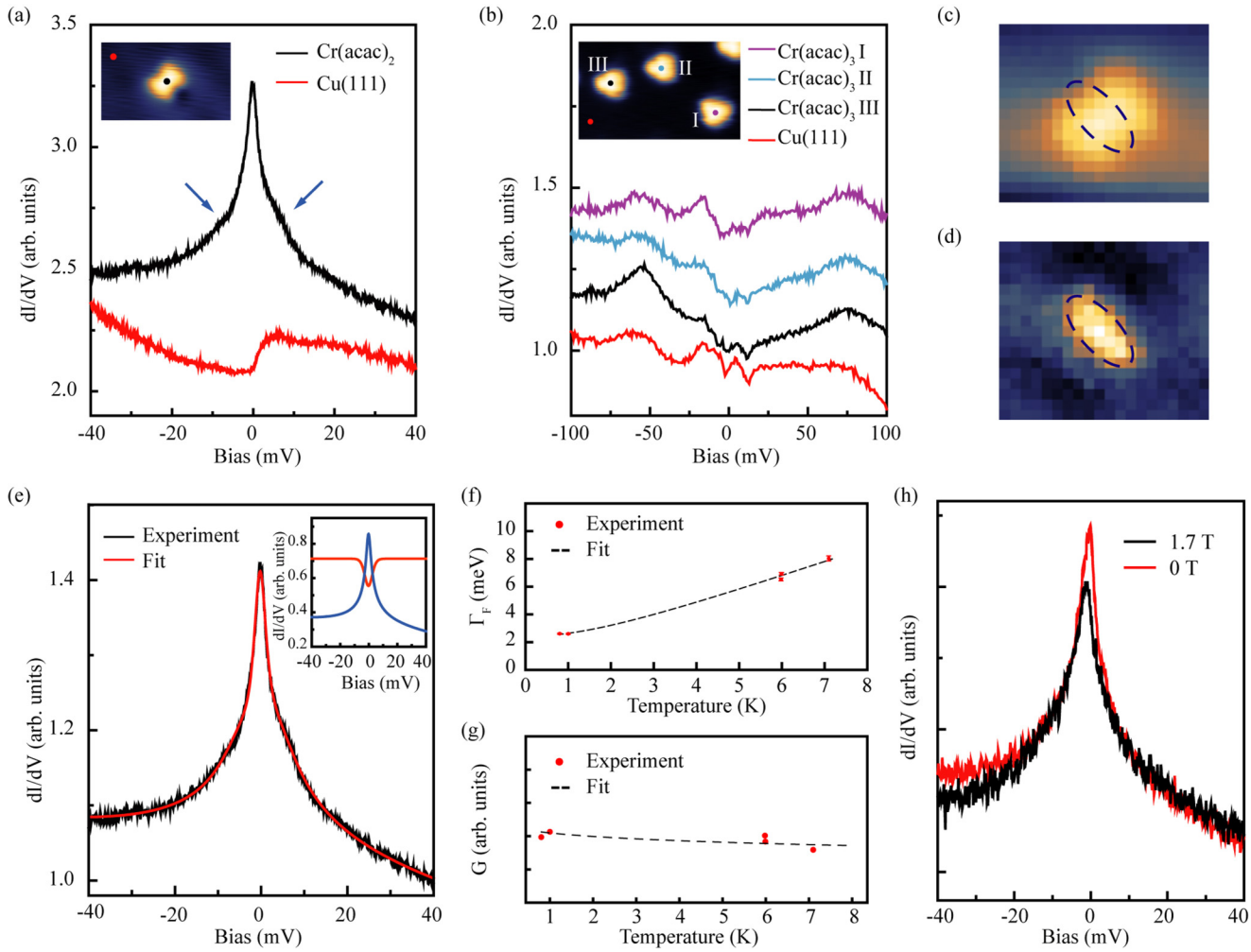

FIG. 2. (a) and (b) dI/dV spectra on dumbbell-shaped $Cr(acac)_2$ and triangular-shaped $Cr(acac)_3$ molecules, respectively. The spectra on Cu(111) surface are also presented for comparison. No background is subtracted. A clear resonance including two shoulders occur on $Cr(acac)_2$ molecules, while the spectra of triangular-shaped $Cr(acac)_3$ molecules are featureless. The blue arrows in (a) mark the position of the two shoulders. The inserted topography images show the tip locations during taking these spectra and are marked in different colored dots. The colors correspond to the curves in each figure. The spectra in (a) were measured at a lock-in modulation of 0.1 mV ($V_{\text{mod}} = 0.1\,\text{mV}$) and frequency of 5.51 kHz ($f_{\text{mod}} = 5.51\,\text{kHz}$) with set point $V = 40\,\text{mV}$, $I = 13\,\text{nA}$. The spectra in (b) were measured at $V_{\text{mod}} = 1\,\text{mV}$ and $f_{\text{mod}} = 2.12\,\text{kHz}$ with set point $V = 100\,\text{mV}$, $I = 300\,\text{pA}$. (c) Scanning tunneling microscopy (STM) topography of a single $Cr(acac)_2$ molecule and (d) corresponding differential conductance map obtained at zero bias, respectively. For every pixel, the feedback loop was opened and dI/dV spectra were recorded. The mapping shows that the position of the Kondo resonance is at the center of the molecule (images size: 2.9×2.4 nm). (e) The fit of the Kondo resonance on the $Cr(acac)_2$ molecule. The black curve presents the experimental data, and the red curve denotes the fit with a Fano-Frota function and two thermally broadened step function. The fitting results are shown as follows: $\Gamma_F = (1.69 \pm 0.02)\,\text{meV}$, $q = 60.6 \pm 4.7$, $\epsilon_{\text{ex}} = (0.76 \pm 0.03)\,\text{meV}$, and $T_{\text{fit}} = (13.0 \pm 0.2)\,\text{K}$. The inset shows the fitting resonance with linear offset (blue curve) and the inelastic steps (orange curve), separately. (f) Temperature dependence of the Kondo resonance. The half widths at half maximum (HWHMs) were extracted from a Frota fit. The black dashed line indicates the fit using the Fermi-liquid model. (g) Temperature dependence of the maximum intensity of the zero-bias Kondo resonance. The black dashed line indicates the fit according to numerical renormalization group (NRG) theory. (h) Magnetic field dependence measurement, $V = 40\,\text{mV}$, $I = 1\,\text{nA}$, $V_{\text{mod}} = 0.1\,\text{mV}$, $f_{\text{mod}} = 5.51\,\text{kHz}$. Some of the spectra are vertically offset for clarity.

rately. To obtain the Kondo temperature, we measured the temperature dependence of the Kondo resonance by tunneling spectroscopy. Figure 2(f) shows the HWHM as a function of temperature in the range from the base temperature of our instrument to 7 K. The resonance width was fitted using the Fermi liquid model [31]: $2\Gamma_F = \sqrt{(\alpha k_B \text{T})^2 + 2(2k_B T_k)^2}$, where α is a free fit parameter, and k_B is the Boltzmann constant. The fit results in a Kondo temperature of $T_k = (19.80 \pm 1.20)\,\text{K}$ and $\alpha = (24.64 \pm 0.47)$. The Kondo temperature is much lower than that of a single Co adatom on an Cu(111) surface [32]. We attribute the relatively low Kondo temperature to the ligands which weaken the coupling between the central magnetic ion and the metal substrate. The value of α deviates strongly from that expected ($\alpha = 2\pi$) based on strong coupling theory. This behavior has been reported by others in similar magnetic molecules on sur-

faces [33]. Figure 2(g) shows the temperature dependence of the peak height of the Kondo resonance together with a fit according to numerical renormalization group (NRG) theory: $G(T) = G(0)[1+(\frac{T}{T_k})^a(2^{1/b}-1)]^{-b}$. The fitting parameters shown in Ref. [34] for a spin of $S = \frac{3}{2}$, i.e., $a = 0.483$ and $b = 0.67$, are adopted. Thus, the only fitting parameter here is the scale of the conductance. As it shows, $G(T)$ fits the theoretical prediction well. Additionally, the broadening of the inelastic step functions of the fit shown in Fig. 2(e) can be expressed as $2\Delta \cong 3.4k_BT_{\text{fit}}$, i.e., $\Delta = (1.90 \pm 0.03)$ meV, which is very similar to that of the Kondo peak $\Gamma_F = (1.69 \pm 0.02)$ meV. This indicates that it is not a thermal broadening but rather a lifetime broadening. This is also expected, as both are caused by the coupling of the local spin to the conduction electrons [35]. Figure 2(h) shows the effect of a magnetic field on the shape of the Kondo resonance. As the HWHM with ∼1.69 meV is much larger than the expected Zeeman splitting of both the Kondo resonance and the inelastic excitations of $\delta E = g\mu_B B$ at 2 T (2 Tesla is the maximal field of our magnet, g is the Landé factor and μ_B is the Bohr magneton), which is of the order of 0.2 meV, we cannot observe the splitting of the Kondo peak or the inelastic excitations for this high lifetime broadening. However, the sharpness of the Kondo peak is indeed reduced upon applying a magnetic field.

Returning to the triangular-shaped $Cr(acac)_3$ molecules, no such features as a Kondo resonance or an inelastic excitation was observed even when investigating several molecules exemplarily shown in Fig. 2(b). To gain signal-to-noise in the dI/dV signal, a 1 mV lock-in modulation ($V_{\text{mod}} = 1$ mV) was used for these spectra trading signal-to-noise for energy resolution. Note that, even at low lock-in modulations ($V_{\text{mod}} \leqslant 0.25$ mV), no Kondo feature or molecular excitation could be observed, and even the second derivative of the tunneling current was featureless (not shown).

To better understand the relation between the point symmetry and the presence of a Kondo resonance, a second $3d$ metal acetylacetonate [$Co(acac)_3$] was studied. As mentioned above, only one type of object could be observed when deposited on Cu(111). These objects consist of two lobes and exhibit twofold symmetry like the dumbbell-shaped molecules observed on the chromium samples. Figure 3(a) shows the topography of these molecules. Threefold symmetric triangles, like those observed on $Cr(acac)_3$ samples, could not be found for Co-acetylacetonates. We infer that, again, these dumbbell-shaped objects represent the divalent $Co(acac)_2$. This is compatible with previous reports, where the $Co(acac)_3$ decomposed upon sublimation [25,26]. To investigate the magnetic behavior of the Co ions, we recorded dI/dV spectra on different $Co(acac)_2$ at the center of the molecules, as displayed in Fig. 3(b). No spectroscopic features, such as a Kondo resonance nor an inelastic excitation could be observed.

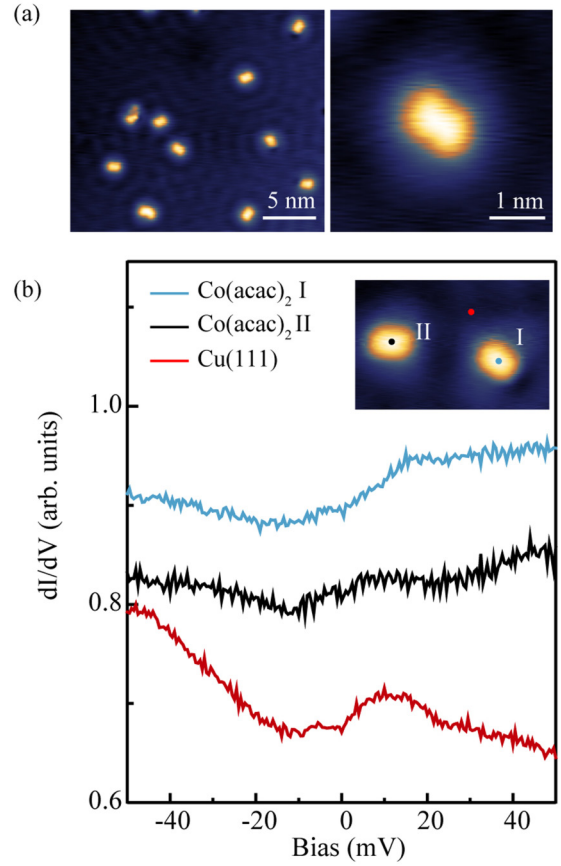

FIG. 3. (a) Topography of the dumbbell-shaped $Co(acac)_2$ molecules ($V = 0.1$ V, $I = 1$nA). Left: Large-scale image. Right: Zoom-in high-resolution image. (b) dI/dV spectra on the dumbbell-shaped $Co(acac)_2$ and Cu(111) surface for comparison. The spectra of molecules do not show a Kondo resonance nor an inelastic excitation. The inset shows the tip locations during the measurements. The marked colored dots correspond to the colored curves. The spectra were measured at $V_{\text{mod}} = 0.5$ mV and $f_{\text{mod}} = 5.51$ kHz with set point $V = 50$ mV, $I = 1$ nA.

IV. DISCUSSION

After presenting the experimental findings, we turn to analyzing the results based on the point symmetry of the individual molecules, the oxidation states of the central ions, and the magnetic properties. To model the effect of geometry, i.e., number of ligands, on the magnetic properties, we represent the spin state of the magnetic ion in the molecules by the effective spin Hamiltonian describing the ZFS. In general, the crystal-field Hamiltonian can be written as

$$\mathcal{H} = \sum_{n=0}^{\infty}\left(\sum_{m=0}^{n} B_n^m O_n^m + \sum_{m=1}^{n} \tilde{B}_n^m \tilde{O}_n^m\right), \tag{3}$$

where O_n^m and $\tilde{O}_n^m$ are Stevens operators, and B_n^m and $\tilde{B}_n^m$ are corresponding coefficients related to the quantum mechanical ZFS [3,19]. Here, B_0^0 is a constant and can be omitted. The operators O_n^m and $\tilde{O}_n^m$ are n th degree polynomials composed of J_z, J_+, and J_- operators (z component, raising and lowering operator), and m indicates the order of ladder operators. Owing to time reversal symmetry, the states with opposite magnetic momentum should be degenerate when no external magnetic field is applied. Thus, only terms with even n are allowed. All terms of $n > 2J$ vanish, where J is the quantum number of total angular momentum, because the operators only act on $2J+1$ states. Similarly, all terms of $n > 2\ell$ vanish,

where ℓ is the orbital quantum number of the open shell of the magnetic ion, i.e., for $\ell = 2$ of the $3d$ states, n is limited to 4. More importantly, all terms vanish that are incompatible with the point symmetry of system. Thus, only terms with $m = 0$, 2, and 4 for twofold symmetry and $m = 0$ and 3 for threefold symmetry are allowed in $3d$ metal system. For this paper, the orbital angular momentum L is quenched for the $3d$ metal such that their magnetic properties arise merely from the total electron spin S, i.e., $J = S$. Finally, in case a vertical mirror plane is present, all conjugate Stevens operators $\tilde{O}_n^m$ vanish. This is the case for the twofold symmetric molecules where the acetylacetonate groups are in one plane.

As a last ingredient, the spin S must be determined. While S is known for the bulk phase of the starting $M(\mathrm{III})(\mathrm{acac})_3$ (M = Cr or Co) complexes, taking away one of the acac ligands potentially changes the oxidation state of the ion M(III) to M(II). Additionally, upon adsorption of the molecules on the Cu(111) surface, charge transfer may arise [9,13]. Unfortunately, STM does not have the capability to directly determine the oxidation state. We, however, will use the results from tunneling spectroscopy to indirectly evidence the oxidation state and thus the spin S.

First, we discuss the case of $\mathrm{Cr(acac)_2}$. We expect that, upon removal of one acac ligand, the oxidation state of Cr(III) changes to Cr(II), but adsorption onto the surface leads to chemisorption and a transfer of one electron from Cr to the Cu substrate [Cr(II) to Cr(III)]. This would lead to the electron configuration of $[\mathrm{Ar}]3d^3$ and a total spin $S = \frac{3}{2}$. Then the Hamiltonian for this twofold symmetric $\mathrm{Cr(III)(acac)_2}$ with one mirror plane can be written as follows:

$$\mathcal{H} = B_2^0 O_2^0 + B_2^2 O_2^2. \tag{4}$$

Since the O_2^2 operator mixes the states with $\Delta S_z = 2$, the four eigenstates can be expressed as linear combinations of $S_z = -\frac{3}{2}$, $\frac{1}{2}$, and $S_z = -\frac{1}{2}$, $\frac{3}{2}$, respectively. As plotted in Fig. 4(a), the system consists of two subsets of states, marked in magenta and blue. Regardless of the precise values of the crystal field parameters B_2^0 and $B_2^2(\neq 0)$, we obtain a ground state Kramers doublet with two states of opposite color. As discussed above, the composition of these two states contains neighboring values of S_z. Thus, single electron scattering by substrate electrons can flip the spin of the molecule between the two degenerate ground states without energy cost, and a Kondo resonance should arise [18]. On top of this, inelastic excitations by the tunneling current may excite the molecule from the ground state doublet to the excited state doublet, which would manifest in the dI/dV spectra as symmetric steps. The experimental results of twofold symmetric $\mathrm{Cr(acac)_2}$ molecules show both expected features [see Fig. 2(e)]. A sketch of the two possibilities of this twofold symmetry case is shown in Fig. 4(a).

Taking a similar line of thought for $\mathrm{Co(acac)_2}$ molecules yields an integer total spin, i.e., $\mathrm{Co}^{3+}([\mathrm{Ar}]3d^6)$ This would allow, depending on the size of the crystal field splitting, Co^{3+} with $S = 0$, 1, and 2. Thus, we expect the following Hamiltonian:

$$\mathcal{H} = B_2^0 O_2^0 + B_2^2 O_2^2 + B_4^0 O_4^0 + B_4^2 O_4^2 + B_4^4 O_4^4. \tag{5}$$

For all three values of S, no Kondo effect is predicted as O_2^2 (and eventually also O_4^4) would mix the otherwise degenerate states with $S_z = \pm 1$ and ± 2 leading to nonmagnetic symmetric and antisymmetric combinations of the S_z components [18]. As a result, only singlet states are left. To be more precise, for $S = 0$, only one nonmagnetic state would arise; for $S = 1$, three nonmagnetic states result; and for $S = 2$, five exist. This situation is sketched in Fig. 4(b). This analysis fully agrees with the absence of a Kondo peak in the dI/dV spectra [see Fig. 3(b)]. As no inelastic excitations were observed [see Fig. 3(b)], our measurements indicate a singlet state, which means the system is in the $S = 0$ diamagnetic state like the bulk counterpart [22]. Nevertheless, it is also possible that the excitations which would arise for $S = 1$ or 2, which are of too low energy for our experimental energy resolution. To conclude this section, the molecules with nonmagnetic singlet ground state are not suited for the application as SMM or quantum bits.

Lastly, for threefold symmetric $\mathrm{Cr(acac)_3}$ with $S = \frac{3}{2}$, the crystalline molecules have already been studied using electron paramagnetic resonance [21]. The crystal field parameters of the model Hamiltonian

$$\mathcal{H} = g\mu_B \boldsymbol{B}\cdot\boldsymbol{S} + D\left[S_z^2 - (1/3)S(S+1)\right] + E\left(S_x^2 - S_y^2\right), \tag{6}$$

were determined to be $|D| = (0.592 \pm 0.002)\,\mathrm{cm}^{-1}$ and $|E| = (0.052 \pm 0.002)\,\mathrm{cm}^{-1}$. Assuming a positive value of D [36], the ground state doublet would consist mainly of the states with $S_z = \pm\frac{1}{2}$. Hence, in STS, one would expect a Kondo resonance with one inelastic excitation at $2D \approx 150$ μeV. While in the bulk phase, a D_3 point-group symmetry is present, and the adsorbed molecules on Cu(111) show a threefold symmetry due to planarization of the molecule upon adsorption. Thus, O_2^2, i.e., the E term in the model above, would vanish in our case, but O_4^0 and O_4^3 would be allowed for $S = 2$ or larger. In the case of no charge transfer, Cr would be in the (III) oxidation state and $S = \frac{3}{2}$, while for the case of a transfer of one electron, Cr would be in the (IV) oxidation state with $S = 1$. In both cases, the Hamiltonian simplifies to

$$\mathcal{H} = B_2^0 O_2^0. \tag{7}$$

Our experimental results showed no Kondo feature or inelastic excitation [see Fig. 2(b)] in this symmetry. Since Kondo resonances are typically easily seen in STS experiments, we may conclude an absence of a Kondo resonance. Inelastic excitations can cause small signals and might be overlooked in experiments. For all cases theoretically expected, one inelastic excitation is predicted, as will be discussed below. Thus, we believe that the amplitude or energy of the inelastic scattering is too small to be observed on the background on the bare Cu(111) spectrum [see Fig. 2(b)]. Therefore, we focus on the Kondo resonance and discuss the different oxidation states.

(1) Charge transfer does not occur. Two different cases can arise for the resulting $S = \frac{3}{2}$ system. As shown in Fig. 4(c), $B_2^0 > 0$ will result in a Kondo effect, while $B_2^0 < 0$ will give an unscreened ground state doublet $|\pm\frac{3}{2}\rangle$. Thus, in this case, due to the absence of a Kondo peak in the experiments, we conclude that the crystal field parameter B_2^0 is expected to be negative.

(2) Charge transfer occurs. Depending on the ligand field parameters, there are two possibilities for the resulting spin

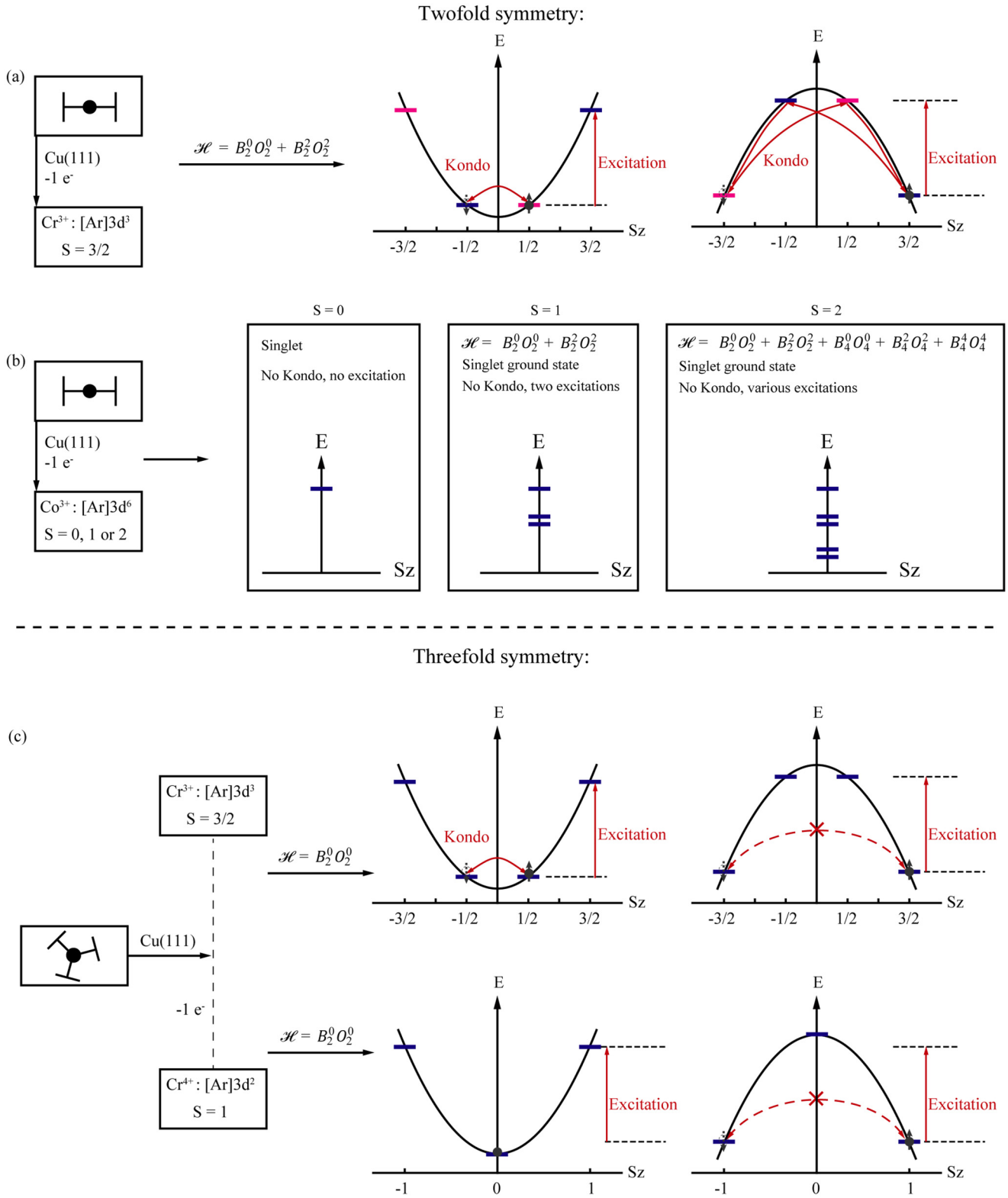

FIG. 4. Overview of the results for Cr- and Co-acetylacetonates adsorbed on Cu(111) surface. For every symmetry and spin state, the effective spin Hamiltonian, the corresponding spin spectrum, and the expected spectroscopic features are denoted. (a) and (b) Different possible cases of twofold symmetric $Cr(acac)_2$ and $Co(acac)_2$ molecules, respectively. (c) With and without charge transfer process, the possible cases of threefold symmetric $Cr(acac)_3$ molecules.

$S = 1$ system: $B_2^0 > 0$ yields a singlet ground state $|0\rangle$, while $B_2^0 < 0$ results in an unscreened ground state doublet $|\pm 1\rangle$. In both cases, no Kondo resonance can be expected, which is consistent with our experimental results. One inelastic excitation is expected but was not observed in the experiment. This can be due to a low excitation energy below the energy resolution of our instrument or due to a small excitation probability leading to too low signal intensity.

V. SUMMARY

Figure 4 summarizes the theoretical expectation for the different systems (symmetry of the crystal field and charge transfer). We conclude that—except for in part missing inelastic excitations—the observations can be broken down and understood in the rather simple framework analyzing the symmetry and electron spin of the molecule. Our results indicate that the twofold symmetric dumbbell configurations are either a Kondo system [$Cr(acac)_2$] or display a nonmagnetic singlet [$Co(acac)_2$] and are thus not suited for application as SMM. Whether threefold symmetric systems are suitable candidates for SMMs crucially depends on the sign of the crystal field parameter B_2^0. These experimental measurements indicate that symmetry plays an essential role in determining the magnetic properties of molecules when adsorbed onto conductive substrates.

ACKNOWLEDGMENTS

T.F. acknowledges funding by the Landesstiftung Baden-Württemberg. W.W. acknowledges funding by the Deutsche Forschungsgemeinschaft (DFG) under the Grant No. WU349/13-1.

[1] L. Bogani and W. Wernsdorfer, Molecular spintronics using single-molecule magnets, Nat. Mater. **7**, 179 (2008).
[2] S. Thiele, F. Balestro, R. Ballou, S. Klyatskaya, M. Ruben, and W. Wernsdorfer, Electrically driven nuclear spin resonance in single-molecule magnets, Science **344**, 1135 (2014).
[3] T. Miyamachi, T. Schuh, T. Markl, C. Bresch, T. Balashov, A. Stohr, C. Karlewski, S. Andre, M. Marthaler, M. Hoffmann, M. Geilhufe, S. Ostanin, W. Hergert, I. Mertig, G. Schon, A. Ernst, and W. Wulfhekel, Stabilizing the magnetic moment of single holmium atoms by symmetry, Nature **503**, 242 (2013).
[4] L. Gu and R. Q. Wu, Origins of Slow Magnetic Relaxation in Single-Molecule Magnets, Phys. Rev. Lett. **125**, 117203 (2020).
[5] J. M. Frost, K. L. M. Harriman, and M. Murugesu, The rise of 3*d* single-ion magnets in molecular magnetism: towards materials from molecules? Chem. Sci. **7**, 2470 (2016).
[6] F. S. Guo, B. M. Day, Y. C. Chen, M. L. Tong, A. Mansikkamaki, and R. A. Layfield, Magnetic hysteresis up to 80 kelvin in a dysprosium metallocene single-molecule magnet, Science **362**, 1400 (2018).
[7] C. Karlewski, M. Marthaler, T. Märkl, T. Balashov, W. Wulfhekel, and G. Schön, Magnetic adatoms as memory bits: a quantum master equation analysis, Phys. Rev. B **91**, 245430 (2015).
[8] G. Czap, P. J. Wagner, J. Li, F. Xue, J. Yao, R. Wu, and W. Ho, Detection of Spin-Vibration States in Single Magnetic Molecules, Phys. Rev. Lett. **123**, 106803 (2019).
[9] U. G. E. Perera, H. J. Kulik, V. Iancu, L. G. G. V. Dias da Silva, S. E. Ulloa, N. Marzari, and S. W. Hla, Spatially Extended Kondo State in Magnetic Molecules Induced by Interfacial Charge Transfer, Phys. Rev. Lett. **105**, 106601 (2010).
[10] P. Wahl, L. Diekhoner, G. Wittich, L. Vitali, M. A. Schneider, and K. Kern, Kondo Effect of Molecular Complexes at Surfaces: Ligand Control of the Local Spin Coupling, Phys. Rev. Lett. **95**, 166601 (2005).
[11] L. Zhang, A. Bagrets, D. Xenioti, R. Korytár, M. Schackert, T. Miyamachi, F. Schramm, O. Fuhr, R. Chandrasekar, M. Alouani, M. Ruben, W. Wulfhekel, and F. Evers, Kondo effect in binuclear metal-organic complexes with weakly interacting spins, Phys. Rev. B **91**, 195424 (2015).
[12] K. Yang, H. Chen, T. Pope, Y. B. Hu, L. W. Liu, D. F. Wang, L. Tao, W. D. Xiao, X. M. Fei, Y. Y. Zhang, H. G. Luo, S. X. Du, T. Xiang, W. A. Hofer, and H. J. Gao, Tunable giant magnetoresistance in a single-molecule junction, Nat. Commun. **10**, 3599 (2019).
[13] J. Hu and R. Wu, Control of the Magnetism and Magnetic Anisotropy of a Single-Molecule Magnet with an Electric Field, Phys. Rev. Lett. **110**, 097202 (2013).
[14] N. Tsukahara, K. I. Noto, M. Ohara, S. Shiraki, N. Takagi, Y. Takata, J. Miyawaki, M. Taguchi, A. Chainani, S. Shin, and M. Kawai, Adsorption-Induced Switching of Magnetic Anisotropy in a Single Iron(II) Phthalocyanine Molecule on an Oxidized Cu(110) Surface, Phys. Rev. Lett. **102**, 167203 (2009).
[15] E. del Barco, A. D. Kent, E. M. Rumberger, D. N. Hendrickson, and G. Christou, Symmetry of Magnetic Quantum Tunneling in Single Molecule Magnet Mn-12-Acetate, Phys. Rev. Lett. **91**, 047203 (2003).
[16] R. Boca, Zero-field splitting in metal complexes, Coordin. Chem. Rev. **248**, 757 (2004).
[17] J. Chen, H. Isshiki, C. Baretzky, T. Balashov, and W. Wulfhekel, Abrupt switching of crystal fields during formation of molecular contacts, ACS Nano **12**, 3280 (2018).
[18] T. Balashov, C. Karlewski, T. Märkl, G. Schön, and W. Wulfhekel, Electron-assisted magnetization tunneling in single spin systems, Phys. Rev. B **97**, 024412 (2018).
[19] K. W. H. Stevens, Matrix elements and operator equivalents connected with the magnetic properties of rare earth ions, P. Phys. Soc. Lond. A **65**, 209 (1952).
[20] M. Marciani, C. Hübner, and B. Baxevanis, General scheme for stable single and multiatom nanomagnets according to symmetry selection rules, Phys. Rev. B **95**, 125433 (2017).
[21] L. S. Singer, Paramagnetic resonance absorption in some Cr^{+3} complexes, J. Chem. Phys. **23**, 379 (1955).
[22] P.-L. Wang, J.-H. Lee, S.-M. Huang, and L.-P. Hwang, Proton spin relaxation in solutions of the complex tris(acetylacetonato)chromium(III), J. Magn. Reson. **73**, 277 (1987).
[23] L. Zhang, T. Miyamachi, T. Tomanić, R. Dehm, and W. Wulfhekel, A compact sub-Kelvin ultrahigh vacuum

scanning tunneling microscope with high energy resolution and high stability, Rev. Sci. Instrum. **82**, 103702 (2011).

[24] M. A. Siddiqi, R. A. Siddiqui, and B. Atakan, Thermal stability, sublimation pressures and diffusion coefficients of some metal acetylacetonates, Surf. Coat. Technol. **201**, 9055 (2007).

[25] G. Beech and R. M. Lintonbon, Thermal and kinetic studies of some complexes of 2,4-pentanedione, Thermochim. Acta **3**, 97 (1971).

[26] A. Rautiainen, M. Lindblad, L. B. Backman, and R. L. Puurunen, Preparation of silica-supported cobalt catalysts through chemisorption of cobalt(II) and cobalt(III) acetylacetonate, Phys. Chem. Chem. Phys. **4**, 2466 (2002).

[27] M. F. Crommie, C. P. Lutz, and D. M. Eigler, Imaging standing waves in a 2-dimensional electron-gas, Nature **363**, 524 (1993).

[28] K. von Bergmann, M. Ternes, S. Loth, C. P. Lutz, and A. J. Heinrich, Spin Polarization of the Split Kondo State, Phys. Rev. Lett. **114**, 076601 (2015).

[29] U. Fano, Effects of configuration interaction on intensities and phase shifts, Phys. Rev. **124**, 1866 (1961).

[30] H. O. Frota, Shape of the Kondo resonance, Phys. Rev. B **45**, 1096 (1992).

[31] K. Nagaoka, T. Jamneala, M. Grobis, and M. F. Crommie, Temperature Dependence of a Single Kondo Impurity, Phys. Rev. Lett. **88**, 077205 (2002).

[32] N. Knorr, M. A. Schneider, L. Diekhöner, P. Wahl, and K. Kern, Kondo Effect of Single Co Adatoms on Cu Surfaces, Phys. Rev. Lett. **88**, 096804 (2002).

[33] S. Mishra, D. Beyer, K. Eimre, S. Kezilebieke, R. Berger, O. Gröning, C. A. Pignedoli, K. Müllen, P. Liljeroth, P. Ruffieux, X. Feng, and R. Fasel, Topological frustration induces unconventional magnetism in a nanographene, Nat. Nanotechnol. **15**, 22 (2020).

[34] J. J. Parks, A. R. Champagne, T. A. Costi, W. W. Shum, A. N. Pasupathy, E. Neuscamman, S. Flores-Torres, P. S. Cornaglia, A. A. Aligia, C. A. Balseiro, G. K. L. Chan, H. D. Abruña, and D. C. Ralph, Mechanical control of spin states in spin-1 molecules and the underscreened Kondo effect, Science **328**, 1370 (2010).

[35] I. Riess and A. Ron, Kondo-resistivity suppression due to inelastic scattering of conduction electrons by magnetic impurities in alloys, Phys. Rev. B **4**, 4099 (1971).

[36] J. Miller, N. Schaefle, and R. Sharp, Calculating NMR paramagnetic relaxation enhancements without adjustable parameters: the spin-3/2 complex Cr(III)$(acac)_3$, Magn. Reson. Chem. **41**, 806 (2003).